

Three-Dimensional Statistics of Radio Polarimetry

Mark M. McKinnon

National Radio Astronomy Observatory, Socorro, NM 87801 USA

ABSTRACT

The measurement of radio polarization may be regarded as a three-dimensional statistical problem because the large photon densities at radio wavelengths allow the simultaneous detection of the three Stokes parameters which completely describe the radiation's polarization. The statistical nature of the problem arises from the fluctuating instrumental noise, and possibly from fluctuations in the radiation's polarization. A statistical model is used to derive the general, three-dimensional statistics that govern radio polarization measurements. The statistics are derived for specific cases of source-intrinsic polarization, with an emphasis on the orthogonal polarization modes in pulsar radio emission. The statistics are similar to those commonly found in other fields of the physical, biological, and Earth sciences. Given the highly variable linear and circular polarization of pulsar radio emission, an understanding of the three-dimensional statistics may be an essential prerequisite to a thorough interpretation of pulsar polarization data.

Subject headings: Methods: statistical – polarization – pulsars: general – radio continuum: general

1. INTRODUCTION

The large photon densities at radio wavelengths, unlike the much smaller densities at much shorter wavelengths, allow the simultaneous detection of the three Stokes parameters which completely describe the polarization of the electromagnetic radiation (Radhakrishnan 1999; Thompson, Moran, & Swenson 2001). The randomly fluctuating instrumental noise introduces a statistical element to the measurements, so a complete and proper interpretation

¹The National Radio Astronomy Observatory is a facility of the National Science Foundation operated under cooperative agreement by Associated Universities, Inc.

of radio polarization observations requires a three-dimensional statistical analysis. Interestingly, but quite understandably, radio astronomers do not fully exploit this unique aspect of radio science, and effectively reduce a polarization measurement to a problem of one or two dimensions by investigating the circular or linear polarization, respectively, on an individual or separate basis.

The polarization signature of the radiation mechanism under investigation usually dictates which Stokes parameters are actually measured. For example, the Zeeman effect produces a distinctive, circularly-polarized signal, and the measurement of a single component of the polarization vector, the Stokes parameter V , is usually sufficient to observe the polarization of the effect. Synchrotron radiation produces significant linear polarization, but no circular polarization (e.g. Rybicki & Lightman 1979), so most polarization observations of synchrotron-emitting sources only utilize the Stokes parameters Q and U . It follows that the measurement of circular polarization is a one-dimensional (1D) statistical problem because only one Stokes parameter is involved. Similarly, the measurement of linear polarization is a two-dimensional (2D) statistical problem because two Stokes parameters are used. The statistics applicable to the measurement of circular and linear polarization are well-understood, and are documented in McKinnon (2002).

Three-dimensional (3D) statistics of radio polarimetry are particularly relevant to pulsar radio emission, where both the linear and circular polarization can be significant and highly variable. The radio emission mechanism of pulsars is not completely understood, and single pulse polarization observations are made in an attempt to understand it. The results of these observations are usually displayed as longitude-dependent histograms of fractional linear polarization, fractional circular polarization, and position angle (e.g. Backer & Rankin 1980; Stinebring et al. 1984) or as joint probability densities of linear polarization and position angle (PA) or of circular polarization and PA (e.g. Cordes, Rankin, & Backer 1978). The histograms and probability densities beautifully illustrate the statistical nature of the emission’s polarization fluctuations and the fascinating orthogonal polarization modes (OPM). However, these display methods, by their very nature, force one to interpret the emission’s linear and circular polarization on a separate basis (e.g McKinnon 2002), and reveal little, if anything, about the association of the two polarizations. The display methods, in effect, betray our reliance upon the familiar, but limited, 1D and 2D polarization statistics. Applying the more general, and more descriptive, 3D statistics to pulsars may be essential to understanding their emission mechanism. One reason why the 3D statistics may not have been applied is it appears they have yet to be determined.

Directional statistics are a subset of the more general 2D and 3D vector statistics, and govern the possible orientations of a vector. They are particularly applicable to experiments

where a vector’s orientation, but not its amplitude, can be measured, such as measurements of the vanishing angles of birds taking flight and measurements of magnetic remanence in rock formations (e.g. Mardia 1972). The statistics’ widespread applicability in biology and the Earth sciences, the pioneering statistical work of R. A. Fisher, and the advent of the modern computer have all contributed to the rapid development of directional statistics over the last 30 years (Fisher, Lewis, & Embleton 1987). Interestingly, directional statistics were originally developed to solve a problem in astronomy. In 1734, Bernoulli used the statistics to prove that the orbital planes of the planets in the Solar System could not be aligned by chance (Mardia 1972, and references therein). The statistics are not widely used in radio astronomy now, but the possibility of their application to radio polarimetry is very intriguing.

The purpose of this paper is to derive and summarize the 3D statistics that are applicable to radio polarimetry. In §2, the statistics of the measured polarization vector are derived for a source of fixed polarization using the statistical model described in McKinnon (2002). The specific cases of no polarization, linear polarization only, and circular polarization only are evaluated. The polarization vector statistics for OPM are derived in §3. The directional statistics of a polarization vector are derived in §4 for the cases of fixed polarization and OPM. The applicability and limitations of the statistics are discussed in §5. The 3D statistics will be applied to polarization observations in a future paper.

2. FIXED POLARIZATION

The polarization of any source of electromagnetic radiation is completely described by the Stokes parameters Q , U , and V . The parameter V describes the circular polarization of the radiation, and the parameters Q and U describe the real and imaginary parts, respectively, of its linear polarization. The Stokes parameters form a right hand, Cartesian coordinate system, and the radiation’s polarization can be represented by a vector in this three dimensional space, which shall be designated as “Poincaré space” in what follows. For the general case of a polarization vector with an amplitude p and an orientation specified by an azimuth ϕ_o and a colatitude θ_o , the circular polarization is $\mu_V = p \cos \theta_o$, and the real and imaginary parts of the linear polarization are $\mu_Q = p \sin \theta_o \cos \phi_o$ and $\mu_U = p \sin \theta_o \sin \phi_o$, respectively.

The Stokes parameters that are actually recorded during an observation include the contributions from the Gaussian instrumental noise of the radio telescope. If X_N is a random variable that represents the instrumental noise, the measured Stokes parameters are (McKinnon 2002)

$$Q = \mu_Q + X_{N,Q}, \quad (1)$$

$$U = \mu_U + X_{N,U}, \quad (2)$$

$$V = \mu_V + X_{N,V}. \quad (3)$$

Thus defined, each of the measured Stokes parameters is a Gaussian random variable with mean μ and standard deviation σ_N , where σ_N is the magnitude of the instrumental noise. Equations 1 through 3 are a set of linear equations that form a simple, statistical model for the polarization measured with a radio telescope. In its simplest form, the model completely ignores any systematic effects such as instrumental imperfections, calibration errors, parallactic angle rotation, interstellar scintillation, and Faraday rotation.

As long as the antenna temperature produced by the radio source is small in comparison to the system temperature of the radio telescope, the instrumental noise in each of the measured Stokes parameters is independent from that in the others. This being the case, the measured Stokes parameters are independent of one another, and their joint probability density is the product of their individual probability densities (i.e. $f_{QUV} = f_Q f_U f_V$). The Stokes parameters can be evaluated in the context of a joint probability density because they can be detected simultaneously at radio wavelengths and thus the polarization state of the radiation can be completely determined at any instant.

The possible amplitudes and orientations of the measured polarization vector can be determined by converting the joint probability density from Cartesian to spherical coordinates. If the random variables x , y , and z represent the measured Stokes parameters Q , U , and V , respectively, the measured amplitude of the polarization vector is $r = (x^2 + y^2 + z^2)^{1/2}$, and its measured orientation² is given by a colatitude of $\theta = \arccos(z/r)$ and an azimuth of $\phi = \arctan(y/x)$. The position angle (PA) of the linear polarization is $\psi = \phi/2$. After converting from Cartesian to spherical coordinates, one can show that the joint probability density governing the measured values of the polarization vector's amplitude and orientation is

$$f(r, \theta, \phi) = \frac{r^2}{\sigma_N^3} \frac{\sin \theta}{(2\pi)^{3/2}} \exp \left[-\frac{(r^2 + p^2)}{2\sigma_N^2} \right] \exp \left\{ \frac{rp}{\sigma_N^2} [\cos \theta_o \cos \theta + \sin \theta_o \sin \theta \cos(\phi - \phi_o)] \right\}. \quad (4)$$

²This nomenclature for orientation angles is consistent with that of traditional, spherical coordinate systems. It is different from the nomenclature used in McKinnon & Stinebring (1998) and McKinnon (2002) where azimuth and PA were denoted by θ and ϕ , respectively.

2.1. No Polarization

If the electromagnetic radiation is not polarized, the amplitude of its intrinsic polarization vector is $p = 0$. From equation 4, the joint probability density for the measured polarization vector is

$$f(r, \theta, \phi) = \frac{r^2}{\sigma_N^3} \frac{\sin \theta}{(2\pi)^{3/2}} \exp\left(-\frac{r^2}{2\sigma_N^2}\right). \quad (5)$$

The distribution of the vector's amplitude is found by integrating the joint probability density over all orientation angles.

$$f(r) = \int_0^{2\pi} \int_0^\pi f(r, \theta, \phi) d\theta d\phi = \frac{r^2}{\sigma_N^3} \sqrt{\frac{2}{\pi}} \exp\left(-\frac{r^2}{2\sigma_N^2}\right) \quad (6)$$

The amplitude distribution is identical in functional form to the Maxwell-Boltzmann distribution for the speed of molecules in an ideal, classical gas. In retrospect, this is not surprising considering that similar assumptions, namely the statistical independence of the Stokes parameters and of the vector components of a molecule's velocity, were made in the derivation. The mean, $\langle r \rangle$, and standard deviation, σ , of the amplitude distribution are

$$\langle r \rangle = 4\sigma_N / \sqrt{2\pi}, \quad (7)$$

$$\sigma = \sigma_N \sqrt{3 - 8/\pi}. \quad (8)$$

The distribution of the vector's orientation is

$$f(\theta, \phi) = \int_0^\infty f(r, \theta, \phi) dr = \frac{1}{4\pi} \sin \theta, \quad (9)$$

which is isotropic.

2.2. Linear Polarization

When the radiation is linearly polarized, the colatitude of the intrinsic polarization vector is $\theta_o = \pi/2$. If the vector azimuth is $\phi_o = 0$, the polarization occurs in the Stokes parameter Q, and the intrinsic Stokes parameters are $\mu_Q = p$ and $\mu_U = \mu_V = 0$. The joint probability density for the measured values of this polarization vector's amplitude and orientation is

$$f(r, \theta, \phi) = \frac{r^2}{\sigma_N^3} \frac{\sin \theta}{(2\pi)^{3/2}} \exp\left[-\frac{(r^2 + p^2)}{2\sigma_N^2}\right] \exp\left(\frac{rp \sin \theta \cos \phi}{\sigma_N^2}\right). \quad (10)$$

The distribution of the vector's amplitude is

$$f(r) = \int_0^{2\pi} \int_0^\pi f(r, \theta, \phi) d\theta d\phi = \frac{r}{p\sigma_N} \sqrt{\frac{2}{\pi}} \exp\left[-\frac{(r^2 + p^2)}{2\sigma_N^2}\right] \sinh\left(\frac{rp}{\sigma_N^2}\right). \quad (11)$$

The amplitude distribution is shown in the top panel of Figure 1 for different signal-to-noise ratios ($s = p/\sigma_N$). As can be seen in the figure, the amplitude distribution is Maxwell-Boltzmann for small s , and resembles a Gaussian when s is large. The mean amplitude is

$$\langle r \rangle = \int_0^\infty r f(r) dr = \sigma_N \sqrt{\frac{2}{\pi}} \exp\left(-\frac{p^2}{2\sigma_N^2}\right) + \left(\frac{p^2 + \sigma_N^2}{p}\right) \operatorname{erf}\left(\frac{p}{\sigma_N \sqrt{2}}\right). \quad (12)$$

In the limiting cases of high and low signal-to-noise ratio, s , the mean amplitudes are

$$\langle r \rangle \simeq p + \sigma_N^2/p, \quad p \gg \sigma_N, \quad (13)$$

$$\langle r \rangle \simeq \sigma_N \sqrt{\frac{2}{\pi}} \left(2 + \frac{s^2}{3}\right), \quad p < \sigma_N. \quad (14)$$

2.3. Circular Polarization

The colatitude of the radiation's polarization vector is $\theta_o = 0$ when it is circularly polarized. The Stokes parameters of the radiation's polarization are $\mu_V = p$ and $\mu_Q = \mu_U = 0$. The joint probability density for the measured values of this polarization vector's amplitude and orientation is

$$f(r, \theta, \phi) = \frac{r^2}{\sigma_N^3} \frac{\sin \theta}{(2\pi)^{3/2}} \exp\left[-\frac{(r^2 + p^2)}{2\sigma_N^2}\right] \exp\left(\frac{rp \cos \theta}{\sigma_N^2}\right). \quad (15)$$

By integrating over all orientation angles, one can show that the distribution of the vector's amplitude is identical to the result in equation 11. Likewise, the mean amplitude of the measured vector is given by equation 12. It follows that one cannot distinguish between linear and circular polarization on the basis of the amplitude distribution alone.

The joint probability density given by equation 15 is independent of and symmetric in azimuth. Therefore, the orientation of the polarization vector varies primarily in colatitude, θ , and is distributed according to

$$f(\theta) = \int_0^{2\pi} \int_0^\infty f(r, \theta, \phi) dr d\phi, \quad (16)$$

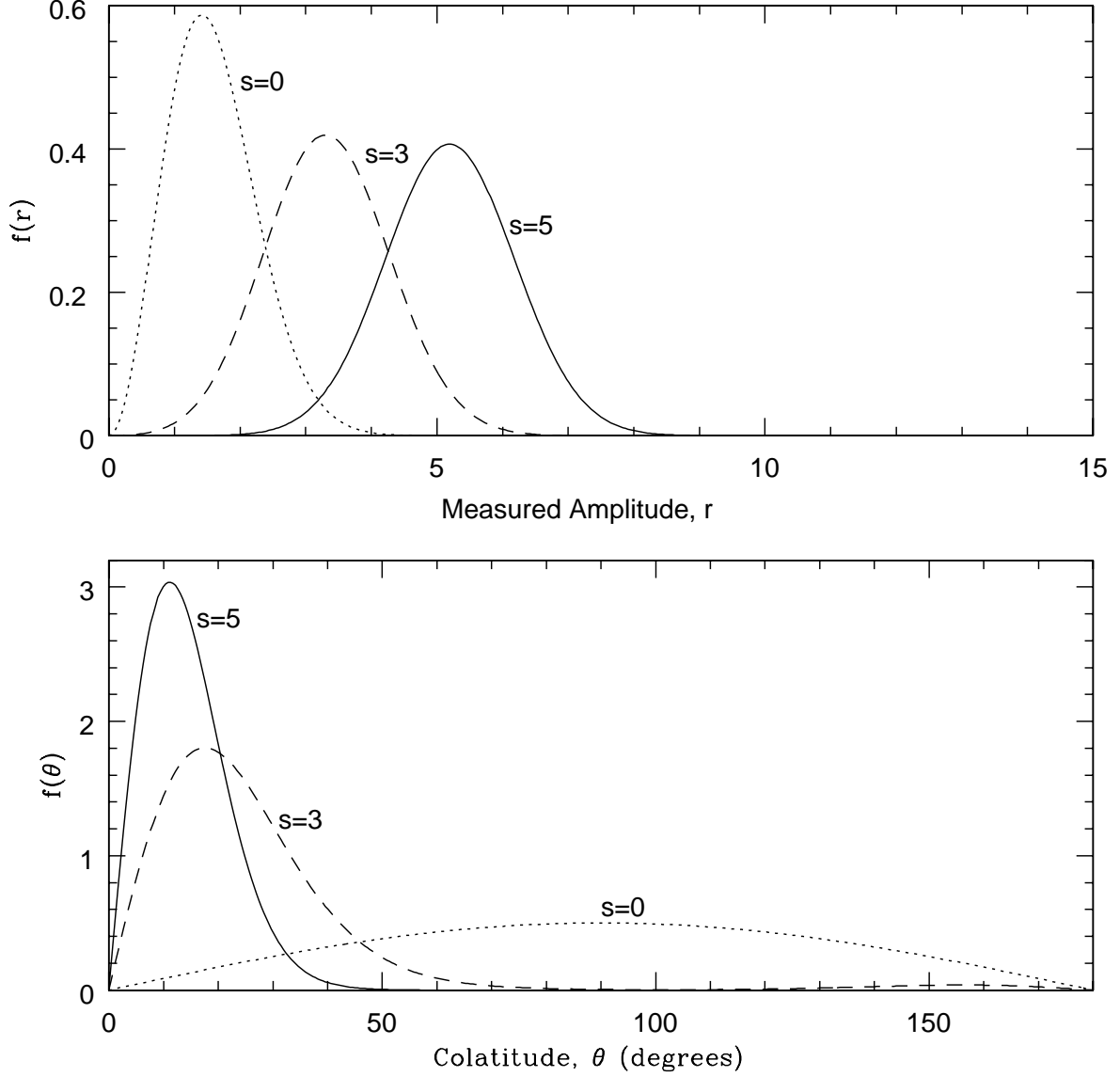


Fig. 1.— Distribution of a polarization vector’s measured amplitude (top panel) and colatitude (bottom panel) for radiation with fixed circular polarization. The distributions are shown for different signal-to-noise ratios, $s = p/\sigma_N$. The colatitude distribution evolves from an isotropic distribution at $s = 0$ to a Rayleigh distribution for large s . The value of the instrumental noise used in the amplitude distributions is $\sigma_N = 1$.

$$f(\theta) = \frac{\sin \theta}{2} \left\{ \exp \left(-\frac{s^2 \sin^2 \theta}{2} \right) \left[1 + \operatorname{erf} \left(\frac{s \cos \theta}{\sqrt{2}} \right) \right] (1 + s^2 \cos^2 \theta) \right. \\ \left. + \sqrt{\frac{2}{\pi}} s \cos \theta \exp \left(-\frac{s^2}{2} \right) \right\}. \quad (17)$$

The colatitude distribution has only one free parameter, s , and is shown in the bottom panel of Figure 1. When s is large ($s \gg 1$), the colatitude distribution approaches the Rayleigh distribution.

$$f(\theta) \simeq s^2 \theta \exp \left(-\frac{s^2 \theta^2}{2} \right) \quad (18)$$

3. ORTHOGONAL MODES OF POLARIZATION

Orthogonal polarization modes are commonly observed in the radio emission from pulsars (e.g. Manchester, Taylor, & Huegunin 1975; Cordes, Rankin, & Backer 1978; Backer & Rankin 1980; Stinebring et al. 1984). In a rather confusing use of the term, the fact that the modes are *orthogonal* actually means their polarization vectors are *antiparallel* in Poincaré space. The modes also appear to occur at the same time (McKinnon & Stinebring 1998, hereafter MS1; McKinnon & Stinebring 2000, hereafter MS2). So although the individual modes may be highly polarized, their simultaneous interaction can cause the observed polarization to be small. To account for the statistical fluctuations observed in the polarization of pulsar radio emission, the amplitudes of the mode polarization vectors can be represented by the random variables X_1 and X_2 (MS1; MS2; McKinnon 2002). The means of these random variables shall be designated as μ_1 and μ_2 , and their standard deviations shall be denoted as σ_1 and σ_2 . Since the observations indicate that the modes occur simultaneously and their polarization vectors are antiparallel, the intrinsic polarization fluctuations occur along a diagonal in Poincaré space. For a diagonal specified by an azimuth ϕ_o and a colatitude θ_o , the observed Stokes parameters can be described by (MS2; McKinnon 2002)

$$Q = \sin \theta_o \cos \phi_o (X_1 - X_2) + X_{N,Q}, \quad (19)$$

$$U = \sin \theta_o \sin \phi_o (X_1 - X_2) + X_{N,U}, \quad (20)$$

$$V = \cos \theta_o (X_1 - X_2) + X_{N,V}. \quad (21)$$

The equations presented so far are valid regardless of the type of random variable that actually describes the amplitudes of the mode polarization vectors. The probability density of

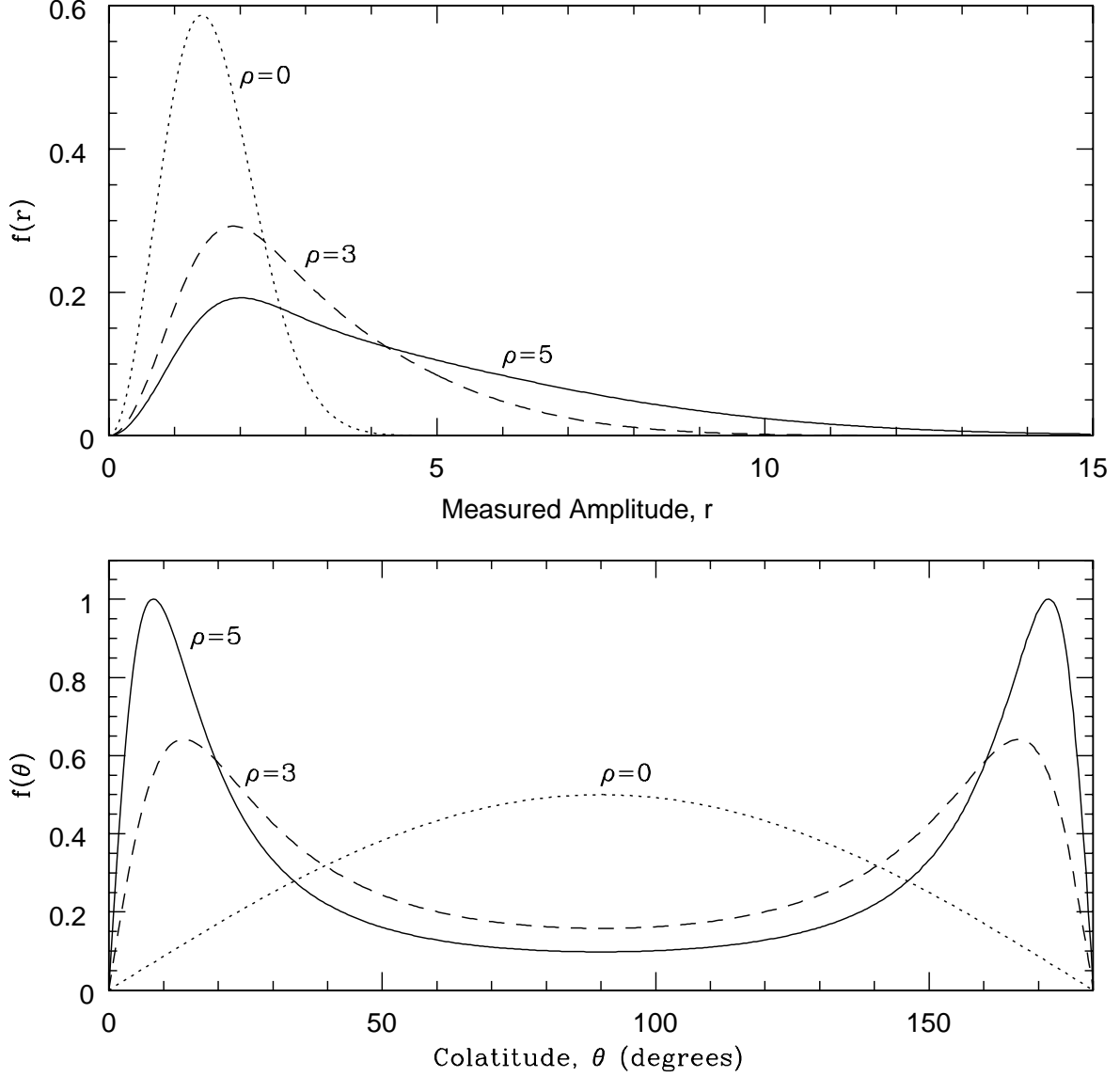


Fig. 2.— Distributions of a polarization vector’s measured amplitude (top panel) and colatitude (bottom panel) when circularly-polarized OPM occurs in the radiation and the mean intrinsic polarization is $p = 0$. In this case, the radiation’s polarization fluctuates, and the different curves represent the distributions expected for different mode fluctuation ratios, ρ . The value of the instrumental noise used in the amplitude distributions is $\sigma_N = 1$.

these random variables must be known before the joint probability density can be derived. In the examples which follow, the mode polarization amplitudes are assumed to be independent, Gaussian random variables.

3.1. Linearly-Polarized Modes

Consider the case when the modes are linearly polarized ($\theta_o = \pi/2$) and their polarization fluctuations occur in Stokes Q ($\phi_o = 0$). In this case, the fluctuations in the measured values of U and V are due to the instrumental noise. Therefore, they are Gaussian random variables with zero means ($\mu_U = \mu_V = 0$) and standard deviations of $\sigma_U = \sigma_V = \sigma_N$. Since the mode polarization amplitudes are assumed to be Gaussian random variables, the measured Stokes Q is also a Gaussian random variable with mean $\mu_Q = p = \mu_1 - \mu_2$ and a standard deviation of $\sigma_Q = (\sigma_1^2 + \sigma_2^2 + \sigma_N^2)^{1/2} \equiv \sigma_N(1 + \rho^2)^{1/2}$. The quantity ρ is a measure of the intrinsic polarization fluctuations relative to the instrumental noise. With these assumptions, the modes will occur at PAs of $\psi = 0^\circ$ and $\psi = 90^\circ$, and will occur with equal frequency if the mode polarizations are the same on average (i.e. $\mu_1 = \mu_2$; $\mu_Q = 0$). The measured Stokes parameters are again independent of one another, and their joint probability density is the product of their individual probability densities (see, also, Appendix A3 of MS1). When the modes have identical mean values ($\mu_1 = \mu_2$; $\mu_Q = 0$), the joint probability density is

$$f(r, \theta, \phi) = \frac{r^2}{\sigma_N^3} \frac{\sin \theta}{(2\pi)^{3/2}} \frac{1}{(1 + \rho^2)^{1/2}} \exp \left[-\frac{r^2(1 + \rho^2) - r^2 \rho^2 \cos^2 \phi \sin^2 \theta}{2(1 + \rho^2)\sigma_N^2} \right], \quad (22)$$

and the distribution of the measured polarization vector's orientation is

$$f(\theta, \phi) = \int_0^\infty f(r, \theta, \phi) dr = \frac{\sin \theta}{4\pi} \frac{1 + \rho^2}{[1 + \rho^2(1 - \cos^2 \phi \sin^2 \theta)]^{3/2}}. \quad (23)$$

3.2. Circularly-Polarized Modes

Although the observations indicate that OPM is predominantly linearly polarized, consider an idealized case where OPM is circularly polarized. The assumption of circularly polarized modes, combined with the observational facts that the modes occur simultaneously and their polarization vectors are antiparallel, means that the intrinsic polarization fluctuations occur only in the Stokes parameter V ($\theta_o = 0$). Again assuming that the mode

polarizations are Gaussian random variables with identical mean values, the joint probability density of the measured polarization vector's amplitude and orientation is

$$f(r, \theta, \phi) = \frac{r^2}{\sigma_N^3} \frac{\sin \theta}{(2\pi)^{3/2}} \frac{1}{(1 + \rho^2)^{1/2}} \exp \left[-\frac{r^2(1 + \rho^2 \sin^2 \theta)}{2(1 + \rho^2)\sigma_N^2} \right]. \quad (24)$$

The assumption of circularly polarized modes introduces azimuthal symmetry to the 3D statistics, and allows for a straightforward, analytical derivation of the amplitude distribution.

$$f(r) = \frac{r^2}{\sigma_N^3} \sqrt{\frac{2}{\pi(1 + \rho^2)}} \exp \left(-\frac{r^2}{2\sigma_N^2} \right) \int_0^1 \exp \left[\frac{\rho^2 r^2 u^2}{2(1 + \rho^2)\sigma_N^2} \right] du \quad (25)$$

The amplitude distribution is shown in the top panel of Figure 2 for different values of ρ . The figure shows that the modes tend to stretch what was originally the Maxwell-Boltzmann distribution of the instrumental noise to a highly asymmetric distribution. The extent of the tail on this distribution increases with the magnitude of the mode fluctuations, ρ .

The azimuthal symmetry of equation 24 also means the orientation of the polarization vector varies primarily in colatitude.

$$f(\theta) = \frac{\sin \theta}{2} \frac{1 + \rho^2}{(1 + \rho^2 \sin^2 \theta)^{3/2}} \quad (26)$$

The colatitude distribution is shown in the bottom panel of Figure 2 for different values of ρ . The distribution is isotropic for $\rho = 0$, and the polarization modes become more obvious as ρ increases. The two peaks in the colatitude distribution do not occur precisely at $\theta = 0, \pi$ because the instrumental noise in Stokes Q and U weights the orientation of the polarization vector towards $\theta = \pi/2$.

Equations 23 and 26 were derived for polarization fluctuations along specific diagonals in Poincaré space. For fluctuations along any other diagonal specified by a colatitude θ_o and an azimuth ϕ_o , the possible orientations of the measured polarization vector are described by

$$f(\theta, \phi) = \frac{\sin \theta}{4\pi} \frac{1 + \rho^2}{[1 + \rho^2 g(\theta, \phi)]^{3/2}}, \quad (27)$$

where

$$g(\theta, \phi) = 1 - [\cos^2 \theta_o \cos^2 \theta + \sin^2 \theta_o \sin^2 \theta (\cos^2 \phi \cos^2 \phi_o + \sin^2 \phi \sin^2 \phi_o)]. \quad (28)$$

4. DIRECTIONAL STATISTICS

The directional statistics of a polarization vector predict the possible orientations of the vector at a given vector amplitude, r_o . They are determined from the 2D or 3D statistics by computing the conditional density of the vector's orientation. In the specific 2D case when only the linear polarization is considered, the conditional density gives the possible PA values on a circle of radius r_o . In the more general 3D case, the conditional density gives the possible vector orientations on a sphere of radius r_o .

4.1. Distribution on a Circle

Figure 3 shows a linear polarization vector in the Q-U plane of Poincaré space, and illustrates the calculation of the PA conditional density. The measured vector is the vector sum of the radiation's polarization and the randomly polarized instrumental noise. The conditional density is the distribution of the measured vector's PAs along the circle of radius, r_o , and is given by

$$f_{\psi|r_o}(\psi) = \frac{f(r_o, \psi)}{f(r_o)}. \quad (29)$$

For the geometry displayed in the figure and noting that ψ is defined on the interval $-\pi/2 \leq \psi \leq \pi/2$, the joint probability density and the amplitude distribution are, respectively

$$f(r, \psi) = \frac{r}{\sigma_N^2} \frac{1}{\pi} \exp \left[-\frac{(r^2 + \mu_Q^2 - 2\mu_Q r \cos 2\psi)}{2\sigma_N^2} \right], \quad (30)$$

$$f(r) = \frac{r}{\sigma_N^2} \exp \left[-\frac{(r^2 + \mu_Q^2)}{2\sigma_N^2} \right] I_0 \left(\frac{r\mu_Q}{\sigma_N^2} \right), \quad (31)$$

where $I_0(x)$ is the modified Bessel function of order zero. From Equations 29 through 31, one can show that the PA conditional density is a von Mises distribution (Mardia 1972; see also MS1) with a dispersion parameter of $b = r_o\mu_Q/\sigma_N^2$.

$$f_{\psi|r_o}(\psi) = \frac{\exp(b \cos 2\psi)}{\pi I_0(b)}, \quad -\pi/2 \leq \psi \leq \pi/2. \quad (32)$$

The PA conditional density is shown in the top panel of Figure 4 for different values of b . It is a uniform distribution at $b = 0$, and is a Gaussian distribution with a FWHM of $(2 \ln 2/b)^{1/2}$ when b is large .

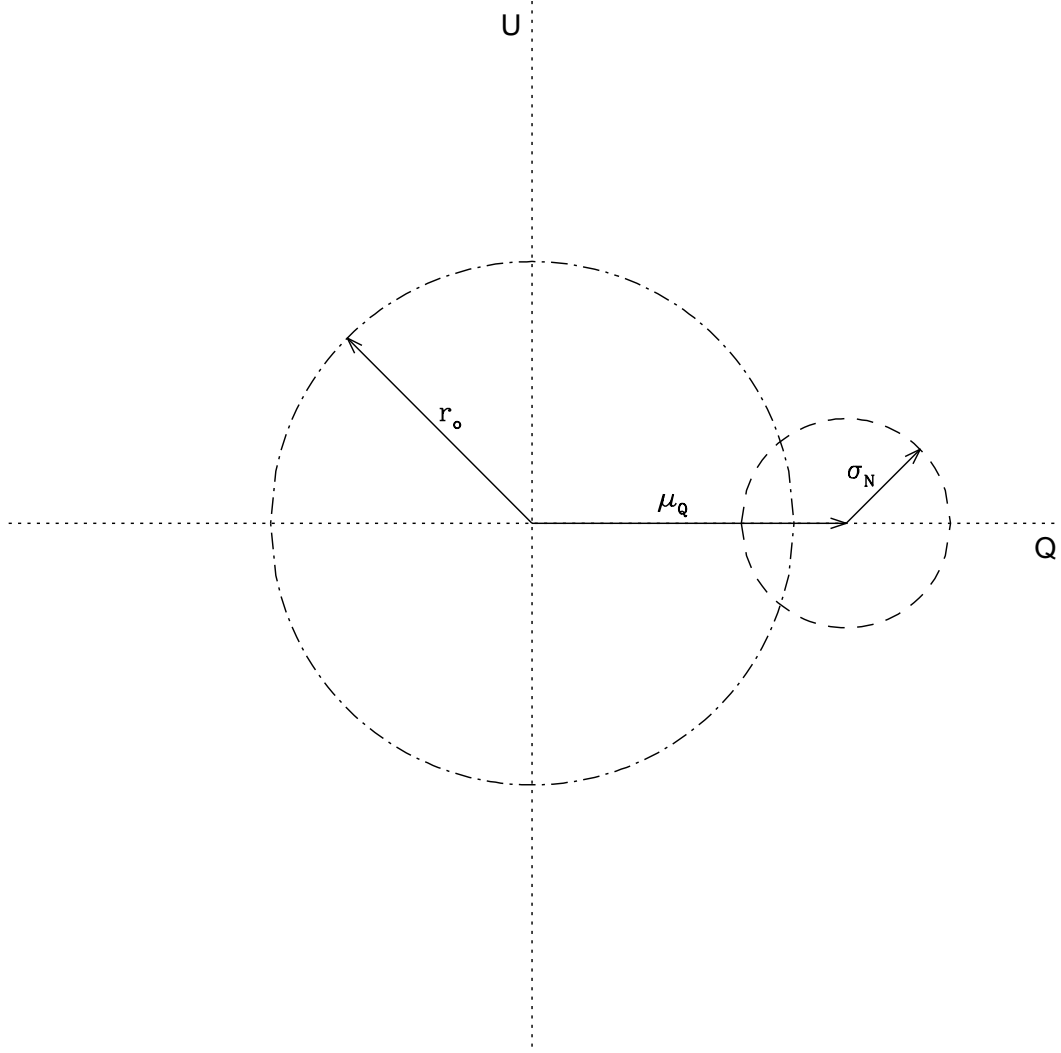


Fig. 3.— Graphical representation of the calculation of the PA conditional density. The radiation’s polarization vector has an amplitude μ_Q and points in the direction of increasing Q in the Q-U plane of Poincaré space. The measured polarization vector includes the instrumental noise, which is a vector with an amplitude characterized by σ_N that can point in any direction (dashed circle). The PA conditional density is the distribution of measured PAs along the circle of radius r_o .

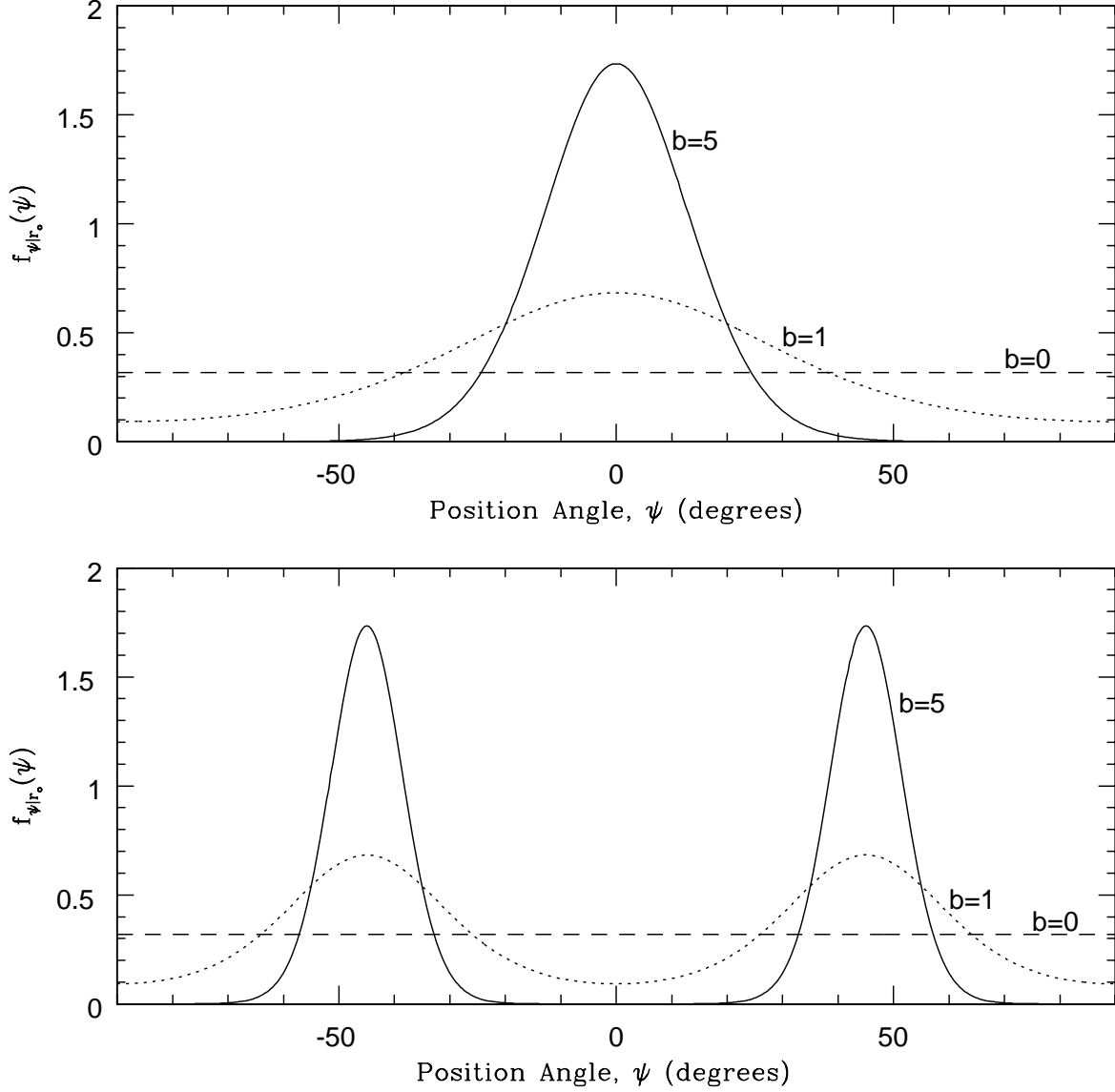


Fig. 4.— Conditional density for the position angle (PA) of a linear polarization vector. When the radiation’s polarization is fixed, the conditional density follows the von Mises distribution (top panel). For linearly-polarized OPM, the conditional density is a bimodal von Mises distribution (bottom panel). The distributions are shown for different dispersion parameters, b .

For linearly-polarized OPM, the joint probability density is (MS1)

$$f(r, \psi) = \frac{r}{\sigma_N^2(1 + \rho^2)^{1/2}} \frac{1}{\pi} \exp \left[-\frac{r^2(1 + \rho^2 \sin^2 2\psi) + \mu_Q^2 - 2\mu_Q r \cos 2\psi}{2\sigma_N^2(1 + \rho^2)} \right] \quad (33)$$

where $\rho = (\sigma_1^2 + \sigma_2^2)^{1/2}/\sigma_N$. When the modes have the same polarization on average ($\mu_Q = 0$), the amplitude distribution is

$$f(r) = \frac{r}{\sigma_N^2(1 + \rho^2)^{1/2}} \exp \left[-\frac{r^2}{4\sigma_N^2} \frac{(2 + \rho^2)}{(1 + \rho^2)} \right] I_0 \left[\frac{r^2}{4\sigma_N^2} \frac{\rho^2}{(1 + \rho^2)} \right]. \quad (34)$$

One can then show that the PA conditional density for linearly-polarized OPM is a bimodal von Mises distribution with a dispersion parameter of $b = r_o^2 \rho^2 / 4\sigma_N^2(1 + \rho^2)$.

$$f_{\psi|r_o}(\psi) = \frac{\exp[b \cos(4\psi)]}{\pi I_0(b)}, \quad -\pi/2 \leq \psi \leq \pi/2 \quad (35)$$

The bimodal von Mises distribution is shown in the bottom panel of Figure 4 for different values of ρ . For display purposes, equation 35 was modified by replacing ψ with $\psi - \pi/4$ so that the modes occur at $\psi = -\pi/4, \pi/4$ in the figure.

Detection thresholds are commonly applied to the measured amplitude of the linear polarization vector before constructing PA histograms (e.g. Stinebring et al. 1984; MS1). The resulting histogram is not an exact replica of the underlying PA distribution, but is more similar to a PA conditional density.

4.2. Distribution on a Sphere

When all three Stokes parameters are measured, the conditional density of a polarization vector's orientation is the distribution of vector orientations on the surface of a sphere, instead of the perimeter of a circle as in § 4.1. As with the PA conditional density, the conditional density of the vector's orientation is calculated from the joint probability density and the amplitude distribution.

For a radiation source with fixed polarization properties, the joint probability density is given by equation 4 and the amplitude distribution is given by equation 11. Since the distribution of the polarization vector's amplitude is independent of its orientation as discussed in § 2, one can use the two equations to show that the conditional density always follows the general Fisher distribution,

$$f(\theta, \phi|r_o) = \frac{f(r_o, \theta, \phi)}{f(r_o)} = \frac{\kappa \sin \theta}{4\pi \sinh(\kappa)} \exp\{\kappa[\cos \theta_o \cos \theta + \sin \theta_o \sin \theta \cos(\phi - \phi_o)]\}, \quad (36)$$

where $\kappa = pr_o/\sigma_N^2$ is a concentration parameter (Fisher, Lewis, & Embleton 1992). As a specific example, $\theta_o = 0$ when the radiation is circularly polarized, and from Equation 36 the conditional density is

$$f(\theta, \phi|r_o) = \frac{\kappa \sin \theta}{4\pi \sinh(\kappa)} \exp(\kappa \cos \theta). \quad (37)$$

Equation 37 is independent of azimuth, as one would expect from the azimuthal symmetry of the problem. Therefore, integration of $f(\theta, \phi|r_o)$ over ϕ yields a factor of 2π , and the resulting colatitude conditional density is $f_{\theta|r_o}(\theta) = 2\pi f(\theta, \phi|r_o)$. The colatitude conditional density is shown in the top panel of Figure 5 for different values of κ . Equation 37 can also be derived directly from the joint probability density in Equation 15 and the amplitude distribution in Equation 11.

For the specific case of circularly-polarized OPM, the conditional density can be found from Equations 24 and 25. The conditional density is a Watson bipolar distribution (Fisher, Lewis, & Embleton 1992) with a concentration parameter of $\kappa = r_o^2 \rho^2 / 2(1 + \rho^2) \sigma_N^2$,

$$f(\theta, \phi|r_o) = \frac{\sin \theta}{4\pi w(\kappa)} \exp(\kappa \cos^2 \theta). \quad (38)$$

Here, $w(\kappa)$ is a normalization factor given by

$$w(\kappa) = \int_0^1 \exp(\kappa u^2) du. \quad (39)$$

This particular distribution is also independent of azimuth, so the colatitude conditional density is again $f_{\theta|r_o}(\theta) = 2\pi f(\theta, \phi|r_o)$. The colatitude conditional density is shown in the bottom panel of Figure 5 for different concentration parameters. Both the Fisher and Watson bipolar distributions become isotropic distributions in the limit $\kappa = 0$.

5. DISCUSSION

The essential point of this paper is microwave polarization measurements can be interpreted in the context of a joint probability density of the Stokes parameters Q, U, and V because the large photon densities at radio wavelengths allow their simultaneous detection. These same photon statistics make coherent phase detection possible and thus the measurement of visibility phase for radio aperture synthesis observations (Radhakrishnan 1999). This important realization allows the derivation of the general 3D statistics for a measured polarization vector. The 3D statistics, in turn, can be used to extract information about the radiation's polarization properties. The statistics derived here are unique to

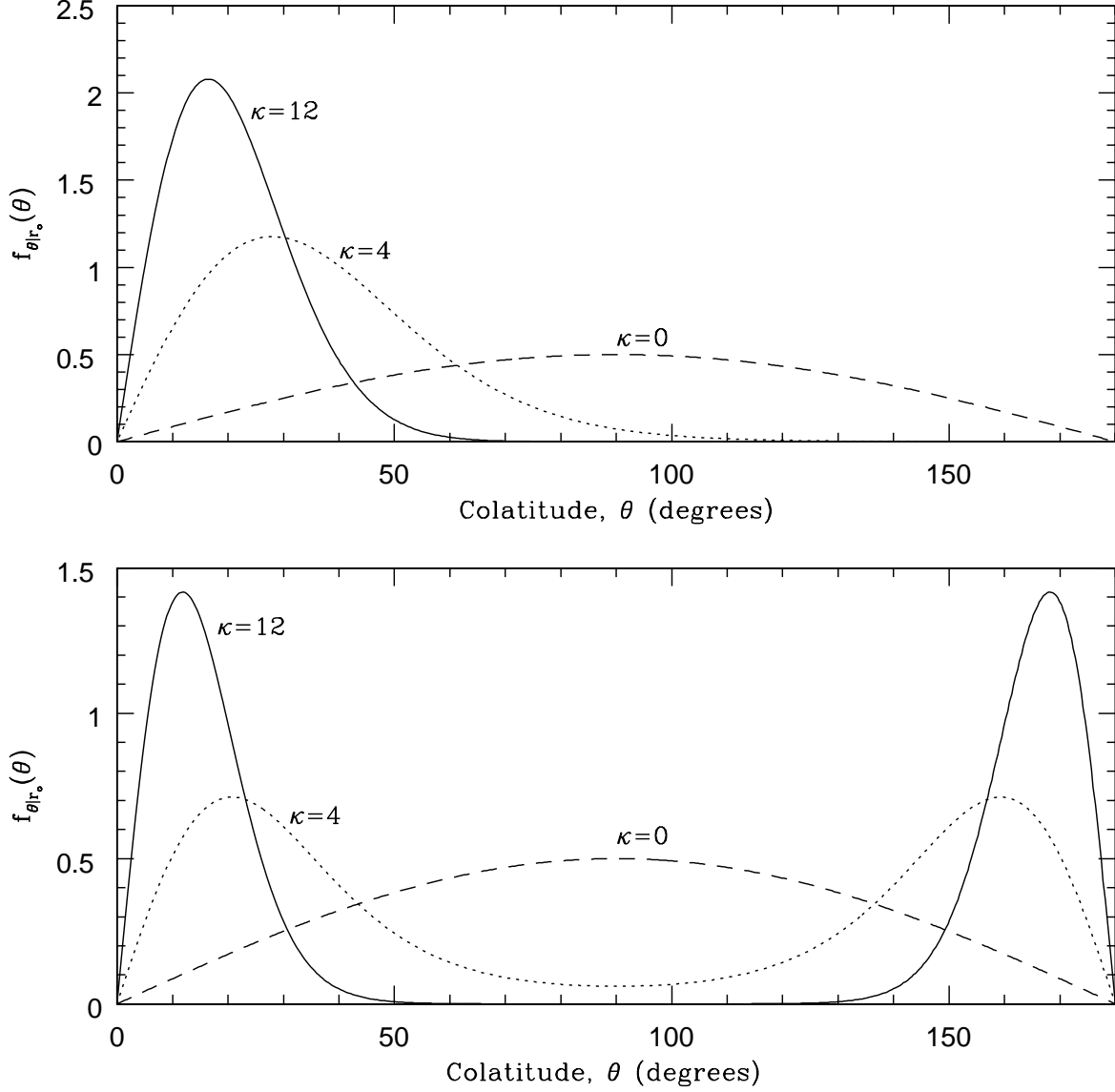


Fig. 5.— Conditional density of a polarization vector’s colatitude, θ , when the radiation is circularly polarized. When the radiation’s polarization is fixed, the conditional density follows the Fisher distribution (top panel). In the case of circularly-polarized OPM, the conditional density follows a Watson bipolar distribution (bottom panel). The distributions are shown for different concentration parameters, κ .

radio polarization measurements, particularly when the radiation’s polarization fluctuates on a timescale comparable to the sampling interval. The statistics may not apply to polarization observations at much shorter wavelengths because the Stokes parameters cannot be measured simultaneously and the polarization state of the radiation may change between consecutive measurements.

The 3D statistics provide the appropriate framework for interpreting observations where both the linear and circular polarization are significant and/or highly variable, as is often the case in pulsar radio emission. Historically, but with some notable exceptions (e.g. Manchester, Taylor, & Huguenin 1975), the linear and circular polarization of individual pulses have been interpreted or evaluated separately, making it difficult to visualize or determine how the polarization vector’s orientation varies from pulse-to-pulse. By applying the 3D statistics derived in this paper, one may be able to make more definite statements about the true polarization state of the radiation.

The statistical model used to derive the polarization statistics accurately describes most radio polarization observations. The model is a set of linear equations that accounts for the radiation’s polarization properties and includes the instrumental noise. The model is valid as long as the telescope system temperature, T_S , is greater than the antenna temperature produced by the radio source, T_A . When T_A becomes comparable with T_S , the instrumental noise is not independent between Stokes parameters and the model is no longer linear.

In deriving the 3D statistics, special emphasis was placed on the specific case of circularly-polarized radiation. This apparent bias does not signify a shortcoming of the statistical model’s ability to describe other types of polarization, but merely highlights the fact that straightforward, analytical solutions can be derived given the azimuthal symmetry provided by the geometry (e.g. Eqns. 17 and 38). Also, the functional form of the distribution of the polarization vector’s orientation is easier to illustrate (e.g. Figs. 1, 2, and 5) for circularly-polarized radiation because the distribution contains only one independent variable (colatitude).

Both the 3D and directional statistics for microwave polarimetry are remarkably similar to those that are relevant in other fields of the physical, biological, and Earth sciences, and it is astonishing that such diverse measurements can be described by the same statistics. For example, measurements of remanent magnetization in rock formations are consistent with the Fisher distribution, and measurements of the intersections between the cleavage and bedding planes of certain types of minerals follow the Watson bipolar distribution (Fisher, Lewis, & Embleton 1987, and references therein). The von Mises distribution can describe the orientations of sand-grains and the vanishing angles of birds taking flight (Mardia 1972, and references therein). These similarities hold great promise for future polarization work

because the mature, rigorous, statistical methods developed in other fields may be applied to radio polarization observations.

REFERENCES

- Backer, D. C. & Rankin, J. M. 1980, *ApJS*, 42, 143
- Cordes, J. M., Rankin, J. M., & Backer, D. C. 1978, *ApJ*, 223, 961
- Fisher, N. I, Lewis, T., & Embleton, B. J. J. 1987, *Statistical Analysis of Spherical Data*, (Cambridge: Cambridge)
- Manchester, R. N., Taylor, J. H., & Huguenin, G. R. 1975, *ApJ*, 196, 83
- Mardia, K. V. 1972, *Statistics of Directional Data*, (London: Academic)
- McKinnon, M. M. 2002, *ApJ*, 568, 302
- McKinnon, M. M. & Stinebring, D. R. 1998, *ApJ*, 502, 883 (MS1)
- McKinnon, M. M. & Stinebring, D. R. 2000, *ApJ*, 529, 435 (MS2)
- Radhakrishnan, V. 1999, in *ASP Conf. Ser. 180, Synthesis Imaging in Radio Astronomy II*, ed. G. B. Taylor, C. L. Carilli, & R. A. Perley (San Francisco: ASP), 671
- Rybicki, G. B. & Lightman, A. P. 1979, *Radiative Processes in Astrophysics*, (New York: John Wiley & Sons), 180
- Stinebring, D. R., Cordes, J. M., Rankin, J. M., Weisberg, J. M., & Boriakoff, V. 1984, *ApJS*, 55, 247
- Thompson, A. R., Moran, J. M., & Swenson, G. W. 2001, *Interferometry and Synthesis in Radio Astronomy*, (New York: John Wiley & Sons)